Simulation of the Radar Cross-Section of Wake Vortices in clear air

Danielle Vanhoenacker-Janvier

D. Vanhoenacker-Janvier[1], K. Djafri[1], R. della Faille de Leverghem*[1], B. van Swieten+[1], F. Barbaresco[2]

[1]*ICTEAM Institute, Electrical Engineering UCL, Maxwell Building, Place du Levant, 3, L05.03.02*
B1348 Louvain-la-Neuve, Belgium, Danielle.vanhoenacker@uclouvain.be, Kahina.djafri@uclouvain.be

[2]*Surface Radar Domain, Technical Directorate Thales Air Systems, Voie Pierre-Gilles de Gennes, F-91470, Limours, France, frederic.barbaresco@thalesgroup.com*

1. Introduction

Real-time sensing of Wake Vortices at take-off and landing is a key issue for the implementation of new air traffic management systems for reduced aircraft separation in favourable weather conditions and for increased air safety. In the framework of SESAR P12.2.2 project, a model has been developed at UCL for the calculation of the radar cross-section of the wake vortices, in a wide frequency range. The first step is the simulation of the evolution of pressure, temperature and humidity versus time, during the landing phase of the aircraft. These parameters are calculated using a pseudo-spectral code developed at UCL and then used for the calculation of the refractive index of the atmosphere under stratified conditions. They are represented in a plane perpendicular to the airplane velocity and evolving with time. The next step is the calculation of the radar cross-section of the various elements of the 3D-grid. The integrand is composed of a rapidly oscillating function in the frequency range of interest. The method of Li [1] has been implemented for the resolution of the integral. The integration method necessitates interpolation between the elements of the grid. Simulations can be calculated for various airplanes weight and span, various speeds, various stratifications of the atmosphere, represented by Brunt-Väisälä constant.

2. Detection of wake vortices using radar

Since the eighties, radar measurements of wake vortices showed an evidence of detection for frequencies going from VHF to X band [2][3][4][5]; these campaigns are described in [6]. Recent measurements with a 35 GHz pulsed Doppler radar [7] or with high resolution 94 GHz radar [8] report the possibility to detect aircraft wake vortices in fog and light rain, with a reasonable power and distances lower than 2 km (500 m for the W band). Barbaresco [9][10] has shown that trials performed with an X-band Doppler radar, are able to continuously detect and characterize the strength as well as to profile wake vortices to a range of 2000m with the radar used.

Lidar is also currently used for the detection and characterization of wake vortices. Radar and lidar are complementary: the lidar is sensitive to the movement of small particles, such as dust, in the vortex and radar is sensitive to pressure and humidity gradients that generate refractive index gradients. The lidar signal is attenuated by fog and rain; the radar signal can be used in fog and also in rain, having in mind that the high frequency radar becomes sensitive to the movement of raindrops of the order of magnitude of their wavelengths [11].

An in depth analysis of the various moments of the radar signal in clear air has been performed by Muschinski [14]; this paper can be useful for application to the wake vortex RCS analysis.

3. Simulation of the refractive index of the wake vortex

The first step is the choice of the mathematical expression of the refractive index of the air in the wake vortex. Various expressions of refractive index exist in the literature; the one of Thayer [12] is currently used for our application. It is a semi-empirical formula valid for frequencies lower than 20 GHz:

$$N = 0.776\frac{p_d}{T} + 1.33\frac{p_{CO_2}}{T} + 0.648\frac{e}{T} + 3.77610^3\frac{e}{T^2} \qquad (1)$$

$$N = \ n - 1 \ 10^6$$

where p_d is the dry air partial pressure [Pa], T is the absolute temperature [K], p_{CO2} is the partial pressure of CO_2 [Pa], e is the water vapor partial pressure [Pa], N is the refractivity and the compressibility factors of dry air and water are assumed to be unity. The various mechanisms responsible for the variation of the refractive index have been analyzed: the radial density gradient in the core of the vortex, the adiabatic compression of the fluid surrounding the core and the contribution of the propulsion from the reactors.

Two mechanisms causing refractive index gradients are generally considered, as presented in [6][10]:

* left UCL, is now with McKinsey&Company
+ left UCL, is now with Tractebel Engineering (GDF Suez)

- The radial density gradient in the vortex cores having a lower pressure and so a lower refractive index than the surrounding medium. This mechanism mainly depends on the airplane type that influences the intensity of the flow.
- The transport of the atmospheric fluid in the oval surrounding the vortices. This mechanism transports the air from one place to another, assuming adiabatic compression when the oval descents and the ambient pressure increases.

The third mechanism is linked to the turbo reactor stream and seems to influence the refractive index in the region close to the aircraft due to high temperature. It will however not be considered in this preliminary model because we are only interested in the vortices a few wingspan away from the airplane. This distance is necessary to ensure the absence of metallic reflections in the main beam and side lobes of the radar antenna.

The dielectric permittivity in the wake vortex is described as

$$\varepsilon_r = \varepsilon_{r,a} + \Delta\varepsilon_r \qquad (2)$$

where $\varepsilon_{r,a}$ is the relative permittivity of ambient air and ε_r the permittivity of the wake vortex. The square root of the permittivity is the refractive index n of air, representing the ambient air when used with "a" subscript. The relative permittivity variation $\Delta\varepsilon_r$ can be linearized as

$$\Delta\varepsilon_r \approx 2\ n - n_a \qquad (3)$$

The accuracy of the linearization has been checked for extreme values of temperature and specific humidity in the troposphere.

Figure 1 shows an example of the evolution of the dielectric permittivity inside the vortex, due to the radial density gradient, for various atmospheric conditions. The US standard atmosphere assumes a pressure of 1013.25 hPa at sea level, a temperature of 285.15 K and a temperature gradient of -6.5 K/km. The characteristic length of the two contra-rotating vortices is b_0, the initial distance between the cores of the vortices. Classically, we can assume, B being the wingspan of the airplane:

$$b_0 = \frac{\pi}{4}B \qquad (4)$$

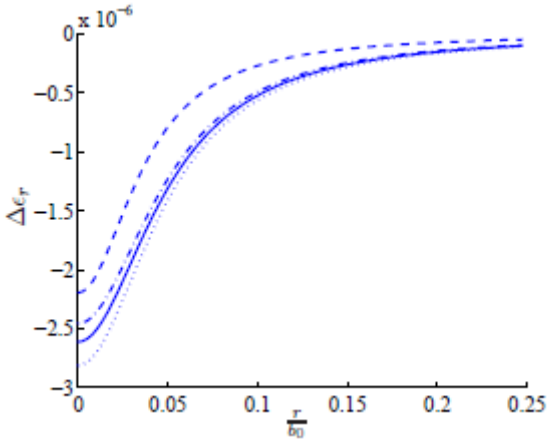

Fig. 1 Distribution of $\Delta\varepsilon_r$ inside the vortex in function of the distance (r) relative to the characteristic length(b_0), for a standard atmospheric profile (——), for a relative humidity of 15% (.-.-), for a temperature of 278.15 K (……) and for a small plane (b_0=35m) (- - -)

The circular movement created by the vortices will mix up the air coming from different altitudes, forming a spiral of refractive index variation. This spiral can be seen in particular cases such as for example when an airplane crosses a thin cloud. Figure 2 provides us a possibility to compare with the simulated $\Delta\varepsilon_r$.

Fig. 2 Airplane crossing a thin cloud. [12]

3.1 Calculation of pressure, temperature and humidity in the wake vortex

The general parameters used for the description of the vortices are the following

$$V_0 \cong \frac{\Gamma_0}{2\pi b_0} \;;\; \Gamma_0 = \frac{Mg}{\rho V b_0} \qquad (5)$$

$$t_0 = \frac{b_0}{V_0} \;;\; \tau = \frac{t}{t_0} \qquad (6)$$

where Γ_0 is the root velocity, V_0 the descent velocity of the vortex pair, b_0 the initial vortex spacing, B the wingspan, V and M are the aircraft velocity and mass, ρ is the air density, g the gravity constant, t_0 is the characteristic time.

The incompressible Navier-Stokes equation, with the Boussinesq approximation, describes the movement. The water vapor concentration obeys to the convection-diffusion equation, being considered as a passive tracer that does not influence the velocity, pressure and temperature fields but is "carried away" by the fluid. The last equation used is the energy equation. 2D pseudo-spectral numerical methods are used for the resolution of the differential equations, so that all the fields have to be periodical and this is not straightforward with stratification of the ambient atmosphere. This imposes the use of some mathematical artifacts to represent periodic pressure, water vapor, velocity and potential temperature. The system of differential equations is then solved by a Runge-Kutta method of order 3. The model for wake vortices necessitates high Reynolds numbers and a very dense mesh. Due to computer limitations, the small scales are not modeled. The introduction of a hyper-viscous term in the equations enables the dissipation of the high wavenumbers, in a way similar to the one used in Large Eddy Simulations. So, the dissipation term only affects the highest wavenumbers. This combined model has been compared to the models proposed by Shariff and shows a good agreement.

3.2 Calculation of the dielectric permittivity in the wake vortex

Using formula (1) and (3), the dielectric permittivity variation can be calculated inside the wake vortex. Figure 3 shows an example of the dielectric permittivity contribution due to the water vapor, 20s after roll up of the vortex. The structure looks similar to the picture of Figure 2. The dielectric permittivity of the vortex has been calculated for various tropospheric parameters, such as relative humidity, temperature gradient, and for various airplanes (A320, A340, A380) having different velocities and altitudes. The simulation extends up to 6 t_0 where t_0 is the characteristic time defined in (6).

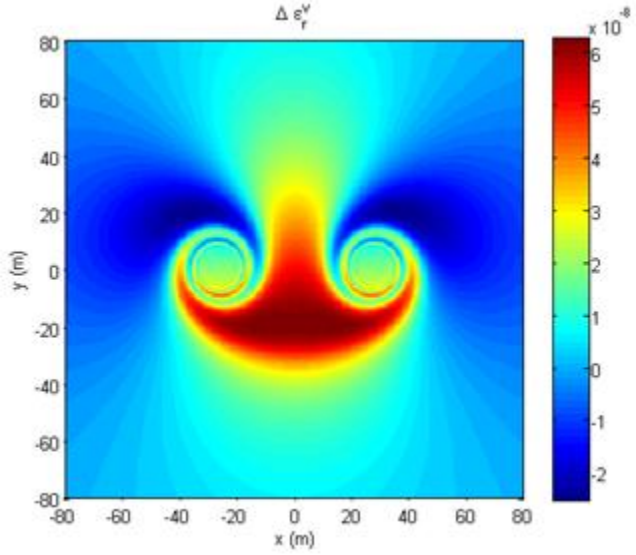

Fig. 3 Example of snapshot of the dielectric permittivity variation $\Delta\varepsilon_r$ due to water vapor.

4. Calculation of the Radar Cross Section

The power received at the radar is given by

$$P_r\ x_r\ = \frac{\omega \varepsilon_0 k_0^2 A^2}{32\pi^2\ x_r\ ^4}\ I^2$$

$$I = \ _V\ \Delta\varepsilon_r f\ x,y,z\ e^{-2jk_0\xi} dV \qquad (7)$$

$$RCS = \frac{k_0^2}{4\pi}\ I\ ^2$$

where ξ is the distance between the receiver and the volume element dV, k_0 is the incident wavenumber, f(x,y,z) is the radiation pattern, A is the amplitude of the incident field and RCS is the radar cross section. I is an oscillating integral because the exponent is rapidly oscillating with position of the volume dV: the wavenumber is very high, especially in X-band which is our frequency of interest. The integration method proposed by Li [1][13] replaces the integral by the

resolution of a system of differential equations. The method has been compared to the one of Shariff and Wray and is more precise. The geometry of the calculation is represented in Figure 4. The volume considered for the integration depends on the antenna beamwidth, the distance between the radar and the target and the time gate. In the example taken, a volume of 40x40x40m has been used. It has to be mentioned that there is no variation of the dielectric permittivity along the x axis for a single calculation due to the 2D resolution of the fluid dynamics equations. This is however not a problem due to the small distance along the x-axis. The same y-z distribution is repeated with a Δx of 1m for the integration along x. The resolution along y and z is 0.5 m.

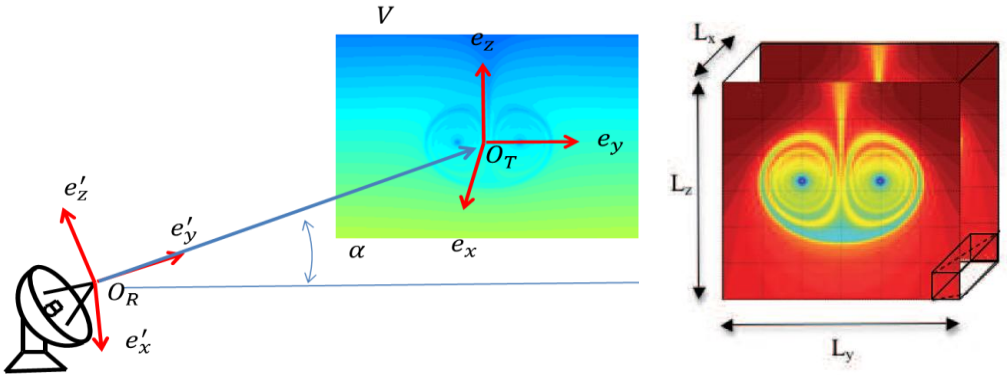

(a) (b)

Fig. 4 (a) Geometry of the radar for the calculation of the RCS, (b) 2D simulation of the dielectric permittivity of the vortex.

The Brunt-Väisälä frequency is defined as

$$N^2 = \frac{g}{\theta_0}\frac{d\theta_a}{dz} \qquad (8)$$

where g is the gravity constant, θ_0 is the potential temperature at the reference level and $d\theta_a/dz$ is the gradient of the potential temperature. It has to be stressed that the Brunt-Väisälä frequency, N^2, is not the square root of the refractivity of the troposphere N. Their notations are kept because they are widely used. The RCS is calculated for an A380 airplane with a velocity of 56 m/s descending in a stable troposphere with a relative humidity of 50%. For comparison purpose, the beam of the antenna is centered in the middle of the vortices as represented in Figure 4 (a). The antenna beam has an elevation of 3 degrees and works at a frequency of 9.1 GHz. The cells represent the successive time gates as shown in Figure 5; eight cells are needed for A380 due to the large wingspan. For comparison purpose, the vortices are assumed to be in a single radar volume. A further analysis of the effect of the position of the vortex inside the radar cell will be performed later.

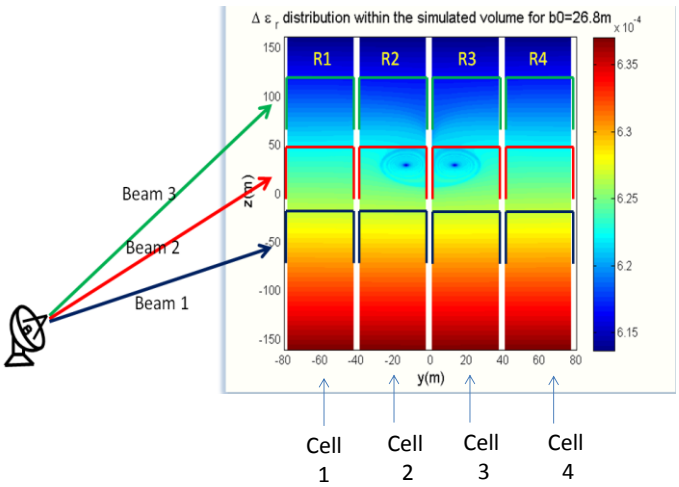

Fig. 5 Geometry used for the comparison between the various radar beams (A320)

A first simulation result is given in Figure 6. It is clearly visible that for an A380 airplane, the vortices are situated in the four central cells (cell 3 to 6) where they influence the RCS measured. The RCS shows an increase with time during the 15 s after the roll up.

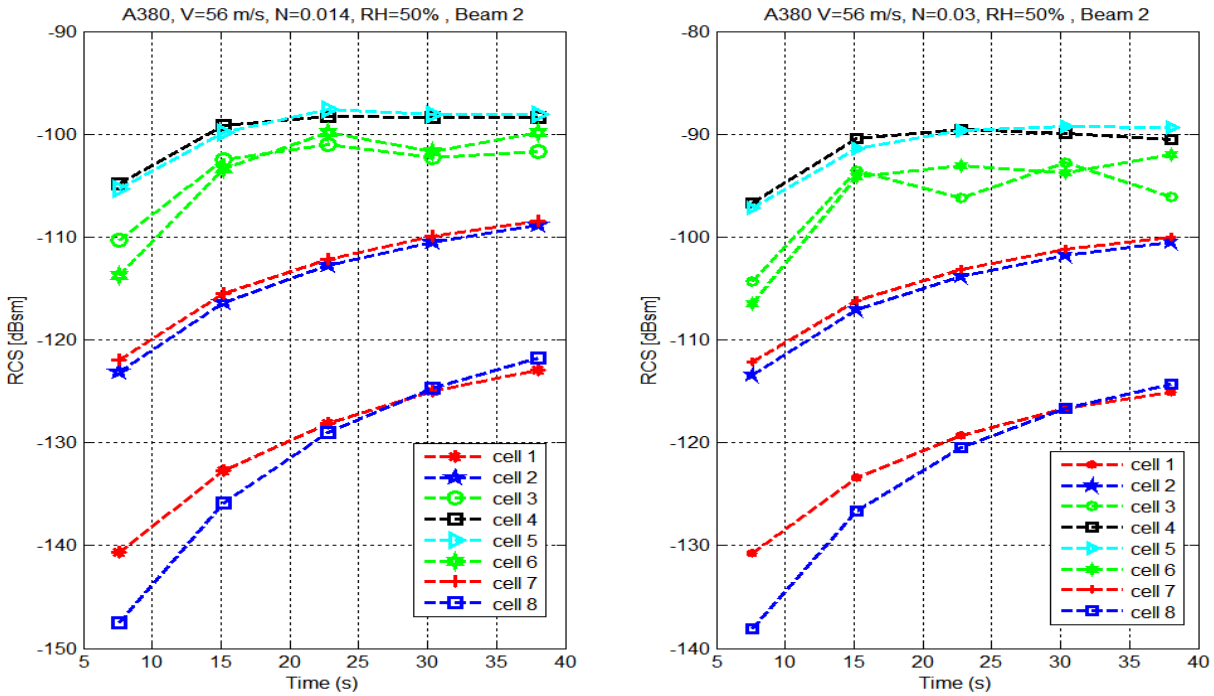

Fig. 6 RCS simulated for a A380 airplane, flying at 100m, with a velocity of 56 m/s, in a stratified air, with 50% relative humidity and two different Brunt-Väisälä frequencies

5 Conclusion

Software has been developed for the simulation of the RCS for a wide frequency range, various airplanes and various tropospheric parameters. A parametric analysis will be performed in order to check the effects of the parameters and further optimize the radar.

Acknowledgement

This research activity has been partially funded by the SESAR P12.2.2 project, which is led by Thales Air Systems. The authors would like to thank Thales Air Systems for the fruitful discussions.

References

[1] Jianbing Li, Xuesong Wang, Tao Wang, 2009, "Delaminating quadrature method for multi-dimensional highly oscillatory integrals", *Applied Mathematics and Computation*, 209(2), pp. 327–338.

[2] Noonkester V. R., Richter J. H., 1980 , "FM-CW radar sensing of the lower atmosphere", Radio Science, vol. 15, pp.337–353.

[3] Chadwick R. B., Jordan J., Detman T., 1984, "Radar cross section measurements of wingtip vortices", Proc. ESA IGARSS 1984, vol. 1, pp. 479–483.

[4] Gilson W. H., 1994, "Aircraft wake RCS measurement", NASA Contractor Rep. 10139, Part 2, pp.603–623.

[5] Shephard D. J., Kyte A. P., Segura C. A., 1994, "Radar vortex measuremetns at F and I band", IEE Colloqium on Radar and Microwave Imaging, London, pp. 7/1-5.

[6] Shariff K., Wray A., 2002, "Analysis of the radar reflectivity of aircraft vortex wakes", J. Fluid Mech, vol. 463, pp. 121-161.

[7] Neec, R. T.; Britt C. L., White J. H., Mudukutore A.; Nguyen C, Hooper B. 2005, "Wake Vortex Tracking Using a 35 GHz Pulsed Doppler Radar", 5th NASA Integrated Communications, Navigation, and Surveillance (ICNS) Conference andWorkshop,.2-5 May 2005, Fairfax, VA, USA, 11 pp.

[8] Seliga T. A., Mead J. B., 2009, "Meter-scale Observations of Aircraft Wake Vortices in Precipitation using a High Resolution Solid-State W-band Radar", 34th Conf. on Radar Meteorology, Williamsburg, USA, 5-9 October 2009, P10.25, 7 p.

[9] Barbaresco F., 2010, "Airport radar monitoring of wake vortex in all weather conditions", Proc. 7th European Radar Conf., Paris, 30 Sept. – 1 Oct. 2010, pp. 85-88.

[10] Barbaresco F., Meier U., 2010, "Radar monitoring of a wake vortex: Electromagnetic reflection of wake turbulence in clear air", Comptes Rendus Physique, Elsevier, vol. 11, pp. 54–67.

[11] Liu Z., Jeannin N., Fabbro V., Wang X., 2011, « Development of a radar simulator for monitoring wake vortices in rainy weather », CIE Intl. Conf. on Radar, Chengdu, China, October 24-27, 2011, 4 p.

[12] Morris S., http://www.airliners.net, April 2009.

[13] Li J., Wang X., Wang T., Xiao S., Zhu M., 2011, "On a quadrature method for oscillatory integrals", Journal of Mathematical Analysis and Applications, vol. 380 (2), pp.467-474.

[14] Muschinski A., 2004, "Local and global statistics of clear-air Doppler radar signals", Radio Science, vol. 39, pp. RS1008, 23 PP., 2004, doi:10.1029/2003RS002908.